

1 **Facile hydrophobic modification of hydrophilic membranes by**
2 **fluoropolymer coating for direct contact membrane distillation**

3

4 Yujun Zhang^{a,b,c}, Jeng Yi Chong^b, Yali Zhao^b, Rong Xu^d, Akihiko Asakawa^e and Rong Wang^{b,c,*}

5

6 ^a Interdisciplinary Graduate Programme, Graduate College, Nanyang Technological University,
7 Singapore 637553, Singapore

8 ^b Singapore Membrane Technology Centre, Nanyang Environment and Water Research Institute,
9 Nanyang Technological University, Singapore 637141, Singapore

10 ^c School of Civil and Environmental Engineering, Nanyang Technological University,
11 Singapore 639798, Singapore

12 ^d School of Chemical and Biomedical Engineering, Nanyang Technological University,
13 Singapore 637459, Singapore

14 ^e AGC Asia Pacific Pte Ltd, Singapore 637143, Singapore

15

16 * Email address: rwang@ntu.edu.sg

17

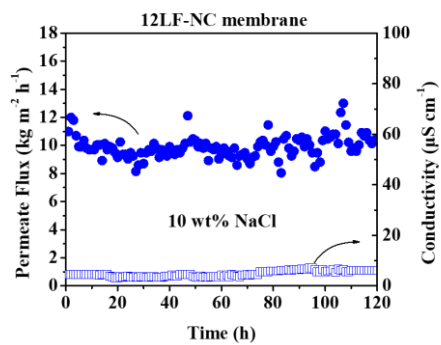
18 **Abstract**

19 Membrane distillation (MD) is a promising desalination technology as it is less sensitive to
20 feed's salinity and can handle high-salinity water. However, the industrial application of MD is
21 restricted by the limited availability of cost-effective hydrophobic membranes. This study
22 developed a simple method to fabricate hydrophobic MD membranes through the coating of a
23 fluoroethylene vinyl ether polymer called LUMIFLON™ LF-200. The fluoropolymer was
24 effectively coated on porous nitrocellulose (NC) and nylon membrane through dip-coating
25 followed by a thermal crosslinking. The coating layer was thin and uniform, covering the
26 surface of the whole membrane matrix, while the high porosity and the microstructure of the
27 membranes were still mostly preserved. After modification, the originally hydrophilic NC and
28 nylon membranes were transformed into hydrophobic, with water contact angles of $\sim 130^\circ$. The
29 12LF-NC membrane showed a high flux of $10.1 \text{ kg m}^{-2} \text{ h}^{-1}$ with salt rejection $>99.99\%$ over
30 120 hours in the direct contact MD fed with 10 wt% NaCl solution, which outperformed the
31 commercial PVDF membrane. This coating method has the potential to modify various
32 substrates to produce MD membranes with good performance, which broadens the availability
33 of appropriate membranes for MD application.

34

35 **Keywords:** Membrane Distillation; Hydrophobic Modification; Desalination; LUMIFLON™
36 LF-200; Nitrocellulose Membrane; Nylon Membrane.

37 **Graphical abstract**



38

39

40

41 **1. Introduction**

42 Seawater desalination is considered as a critical approach to address the increasingly serious
43 water scarcity problem because of the unlimited and renewable seawater from the ocean [1].
44 Today, the most prevailing seawater desalination technology is reverse osmosis (RO), which
45 accounts for 69% of desalinated water production [2]. However, as it is driven by the pressure
46 difference across the membranes, the RO process is often restricted by the high operating
47 pressure when the feed solution becomes concentrated. The water recovery of conventional RO
48 process is normally limited within 50%, with the seawater feed concentrated to ~7 wt% solute
49 concentration and an operating pressure of 55-70 bar [1, 3]. A higher operating pressure may
50 not be cost effective and the current thin-film composite RO membranes could not withstand
51 ultrahigh pressure [4, 5]. Furthermore, the disposal of the unmanageable brine can be a problem
52 in the aspect of economy and environment concerns [6].

53

54 **Membrane distillation (MD), a thermal-driven process, has a significant advantage over RO in**
55 **treating high-salinity solutions. As the water permeation is driven by the partial vapor pressure**
56 **difference across the membrane, MD is generally insensitive to feed salinity [7-11]. For**
57 **example, some studies have applied MD to separate hypersaline water with an NaCl**
58 **concentration up to 20-25 wt% and the process could still achieve excellent rejection of >99.9%**
59 **[12-14]. MD has been demonstrated as a promising technology in volume reduction and mineral**

60 recovery from high-salinity feeds, and also a potential technology to achieve minimum or zero
61 liquid discharge. However, the available commercial membranes customized for MD are
62 relatively limited. MD requires hydrophobic porous membranes and the most popular materials
63 are hydrophobic polymers such as polypropylene (PP), polytetrafluoroethylene (PTFE) and
64 polyvinylidene fluoride (PVDF) [15]. Among them, PTFE and PP are difficult to fabricate via
65 the common non-solvent induced phase inversion method due to their strong solvent-resistance.
66 The commercial PP and PTFE membranes are often fabricated by traditional stretching
67 technology and have a symmetric structure, a relatively large pore size (typically 0.2-20 μm)
68 and wide pore size distribution, which may result in a low wetting resistance [16, 17]. Currently,
69 there is very few improving methods, which may require blending additional additives and
70 involve with high temperature $\sim 400\text{ }^\circ\text{C}$ [18-21]. On the other hand, although PVDF membranes
71 can be fabricated via phase separation and have a more controllable pore size, the majority of
72 commercial PVDF membranes have a limited hydrophobicity as they are normally made for
73 conventional membrane filtration processes. In addition, the fluorinated polymers (i.e. PVDF
74 and PTFE) are usually more costly than the non-fluorinated ones [22, 23].

75

76 For the sake of reducing the cost and expanding the availability of MD membranes, the less
77 hydrophobic or hydrophilic polymeric microfiltration/ultrafiltration membranes can be
78 considered. Although these membranes are unsuitable for MD in terms of wettability, they may

79 have favourable properties such as high porosity and suitable pore structure. Moreover, they
80 can be cost-effective and more flexible in processing compared with the conventional
81 hydrophobic membranes. Transforming the wettability of these membranes to hydrophobic can
82 significantly expand the variety of applicable MD membranes, as well as reducing the cost of
83 MD membrane manufacturing. Several hydrophobic modification methods have been carried
84 out to a wide range of hydrophilic polymeric membranes, including polysulfone (PSf),
85 polyimide (PI), poly(amide-imide) (PAI), poly(etherimide) (PEI), polyacrylonitrile (PAN),
86 polyvinyl chloride (PVC), polyethersulfone (PES), polyamide (PA), cellulose acetate (CA) and
87 nitrocellulose (NC). The existing methods can be classified as increasing roughness via special
88 treatment like vapour-induced phase separation (VIPS) and plasma treatment [24, 25], and
89 decreasing surface energy either during fabrication or as post-treatment [26]. Nevertheless,
90 some of these methods need specific treatments (i.e. UV, plasma), which are unsuitable for
91 large-scale production. Also, most of the previous methods could not obtain membrane with
92 high hydrophobicity with water contact angle $>120^\circ$ facilely and efficiently.

93

94 In this study, a simple and time-saving hydrophobic modification method was developed with
95 a fluoroethylene vinyl ether (FEVE) resin. The modification was conducted via direct and
96 convenient dip coating of the FEVE polymer and followed by a crosslinking step carried out at
97 low temperature or even room temperature to ensure the stability of coating layer. In this work,

98 two types of hydrophilic membranes were used for the hydrophobic modification. First, NC
99 membranes with a high porosity and low price were first studied and the optimum coating
100 conditions were developed. Then, the FEVE polymer was coated on nylon membranes to
101 evaluate the versatility of this modification method. A series of characterisations were carried
102 out to investigate the membranes' hydrophobicity, morphologies and chemistry. Following that,
103 MD experiments in direct contact mode (DCMD) were conducted to explore the potential of
104 the modified NC and nylon membranes in the desalination of salty water with different salt
105 concentrations of up to 10 wt%. The permeate flux and product quality were compared with
106 commercial PVDF membrane. This work demonstrated a facile and widely applicable
107 hydrophobic modification method to produce MD membranes with high performance for the
108 desalination of highly salty water.

109

110 **2. Experimental**

111 **2.1. Materials**

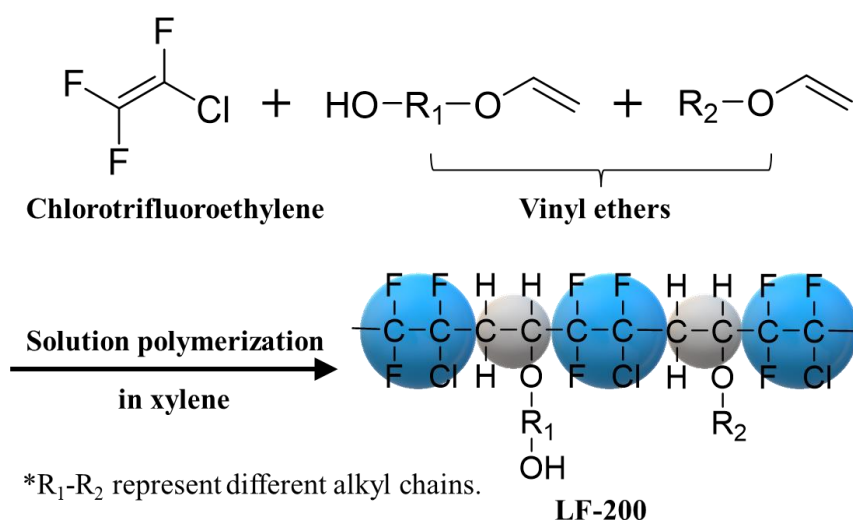
112 A FEVE resin product, LUMIFLON™ LF-200, was supplied by AGC company and its
113 crosslinker, Desmodur® N3300 was supplied by Covestro AG. Xylene (C_8H_{10} , $\geq 98.5\%$ xylenes
114 + ethylbenzene basis) and sodium chloride ($NaCl$, $\geq 99.0\%$) were bought from Sigma-Aldrich
115 (Singapore). All chemicals were used as received. Commercial flat-sheet nylon membranes
116 (mean pore size = $0.2 \mu m$) and NC membranes (mixed cellulose esters, mean pore size = 0.22

117 μm) used as the substrates were purchased from Sterlitech (USA) and Merck Millipore (USA),
118 respectively. PVDF membranes (mean pore size = $0.2 \mu\text{m}$) were obtained from Merck Millipore
119 for a comparative study. Deionized water was produced by a Milli-Q[®] system of Merck
120 Millipore.

121

122 **2.2. Membrane modification**

123 LUMIFLON is a type of FEVE copolymer, which is synthesized by chlorotrifluoroethylene and
124 alkyl vinyl ether through solution polymerization in xylene. Different vinyl ethers, such as ethyl
125 vinyl ether, cyclohexyl vinyl ether and hydroxy butyl vinyl ether can be used in synthesis to
126 introduce different properties to LUMIFLON. Specifically, LUMIFLON LF-200 has a hydroxyl
127 value of 52 mg (KOH)/g polymer, and its structure can be illustrated as Fig.1. The rich -OH
128 functional groups in LF-200 allow its crosslinking with polyisocyanate groups in N3300 to
129 form strong urethane bonds, imparting the coating good chemical stability and durability.
130 Besides, the use of nonpolar solvent, xylene can prevent the damage of the membrane substrates.



131

132 **Fig. 1.** Synthesis process and polymer structure of LF-200.

133

134 To conduct the modification, a coating solution with certain amount of LF-200 and N3300 in

135 xylene was first prepared followed by a vigorous stirring for 15 min at 60 °C. The concentration

136 of LF-200 was designed as 6, 9, 12, 15 wt% in order to optimize the coating effectiveness, and

137 the amount of N3300 was fixed as 17.8 wt% of LF-200 according to the stoichiometric number

138 of functional groups. After getting a homogenous solution, the pristine nylon or NC membrane

139 was dipped in the coating solution for 10 min to ensure the penetration of the coating solution

140 into the membrane substrates and the complete wetting of membrane pores. After that, the

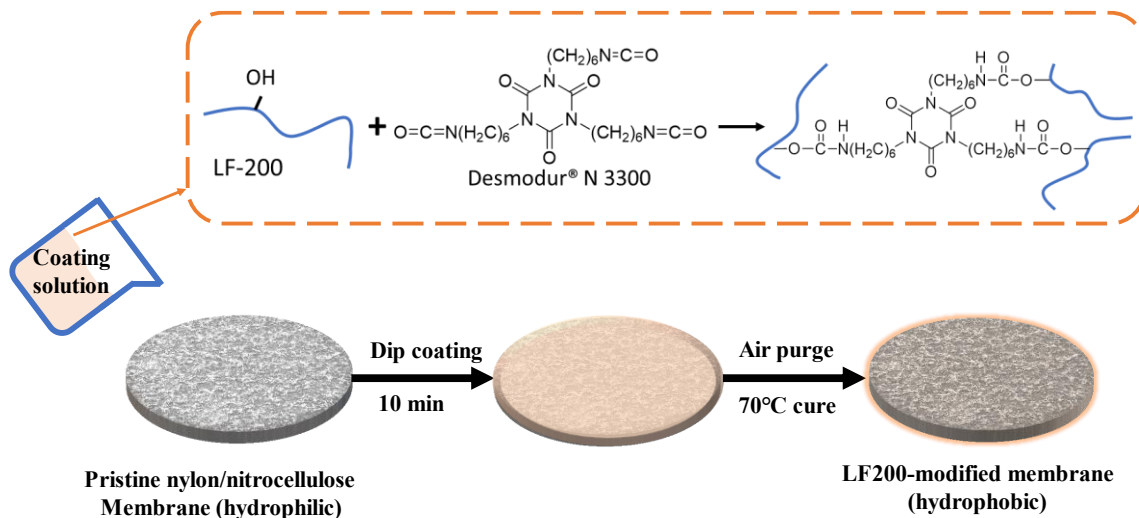
141 membrane was quickly taken out and air-purged for 3 min to remove the residual coating

142 solution as well as accelerating the xylene evaporation. Lastly, the coated membrane was cured

143 at 70 °C in an oven overnight. The coated membrane was named as nLF-NC/nylon, in which n

144 represents the LF-200 concentration (6, 9, 12, 15 wt%) and NC/nylon means the substrate

145 material.



146

147 **Fig. 2.** Schematic of LF-200 crosslinking mechanism and dip coating procedure.

148

149 2.3. Membrane characterizations

150 The morphologies of membrane surface were studied by field emission scanning electron

151 microscope (FESEM, JSM-7200F, JEOL, Japan) and the fluorine scanning spectra of

152 membrane cross-section was obtained by energy-dispersive X-ray (EDX) in low vacuum mode

153 at 10 kV. All membrane samples were sputtered by a thin layer of platinum before FESEM and

154 EDX tests. The surface roughness and topography of the respective membranes was

155 characterized through an atomic force microscope (AFM) (XE-100, Park Systems, Republic of

156 Korea). The average surface roughness (R_a) illustrated the roughness of the membrane surface.

157

158 To confirm the successful modification of LF-200, the surface compositions of pristine and

159 modified NC membranes were analysed by X-ray photoelectron spectrometer (XPS, AXIS

160 Supra, Kratos Analytical, Japan) with monochromatic Al-K α X-ray source ($h\nu = 1486.6$ eV).
161 The water contact angles (WCA) of the modified membranes were measured by a goniometer
162 (Contact Angle System OCA 15EC, DataPhysics, Germany) and compared with the pristine
163 membrane. During each test, a water droplet with volume of 3 μ l was dropped onto the
164 membrane surface and WCA was measured after 3 min. Each sample was tested for 5 times in
165 different positions.

166

167 The mean pore size of the pristine and modified membranes was measured by a capillary flow
168 porometer (CFP 1500A, Porous Material. Inc., USA). Prior to the measurement, the membrane
169 sample was wetted by Galwick[®] ($\gamma \approx 15.9$ mN/m) and nitrogen was used as the displaced gas.
170 Liquid entry pressure (LEP) was tested in a dead-end filtration cell, where pure water was
171 pressurized by nitrogen with a gradually increased pressure (0.2 bar). The pressure when the
172 first droplet spilled out from the cell was recorded as LEP.

173

174 The membrane surface porosity (ε_s , %), considered as the ratio of open pore area on the surface,
175 was calculated from the surface FESEM graph with a magnification of 5000 times. The
176 membrane bulk porosity (ε_b , %), defined by the ratio of pore volume to the matrix volume, was
177 measured by weighing the pristine membrane and membrane wetted by IPA. As the coating
178 layer was extremely thin, so the effect of coating layer was eliminated, and the calculation was

179 based on Eq. (1):

$$180 \quad \varepsilon_b = 100 \times \frac{(w_w - w_d)/\rho_{ipa}}{(w_w - w_d)/\rho_{ipa} + w_d/\rho_m} \quad (1)$$

181 where w_w and w_d are the weight of dry and wet membrane, ρ_{ipa} and ρ_m are density of IPA and
182 the membrane substrate material, respectively.

183

184 **2.4. DCMD performance tests in saline solution**

185 A lab-scale test rig was used to test the desalination performance of modified membranes in a
186 DCMD configuration. The tested membrane was fixed in a stainless-steel membrane cell with
187 an effective area of 12.56 cm². Feed stream with different concentrations of NaCl was circulated
188 on the feed side by a peristaltic pump (Masterflex, Cole-Parmer, USA) with a flowrate of 220
189 ml min⁻¹. Milli-Q[®] water was circulated on the permeate side with a flowrate of 120 ml min⁻¹.
190 The inlet temperatures of the feed and permeate streams were kept constant at 60 ± 0.5 °C and
191 20 ± 0.5 °C, respectively. The overflow from permeate reservoir was collected and weighted
192 automatically by an electrical balance. In the long-term test, the collected permeate was
193 returned to the feed tank every 24 hours in order to maintain the stable conductivity of the feed
194 solution. The water tanks and tubing were covered with insulating materials to reduce heat loss.
195 The permeate flux (J , kg m⁻² h⁻¹) and salt rejection (R) were calculated using Eq. (2) and Eq.
196 (3):

$$197 \quad J = \frac{m}{A \cdot \Delta t} \quad (2)$$

198
$$R = \left(1 - \frac{C_p}{C_f}\right) \times 100\% \quad (3)$$

199 where m is the mass of the collected product (kg), Δt is the time interval (h). C_p and C_f are the
200 concentrations of permeate and feed streams, respectively. After the long-term experiment,
201 respective membranes were washed thoroughly in water with ultrasonication for 10 min and
202 then fully dried in a 60 °C oven. The surface morphologies and WCAs on the feed side of the
203 membranes were tested again to evaluate the stability of the hydrophobic coating.

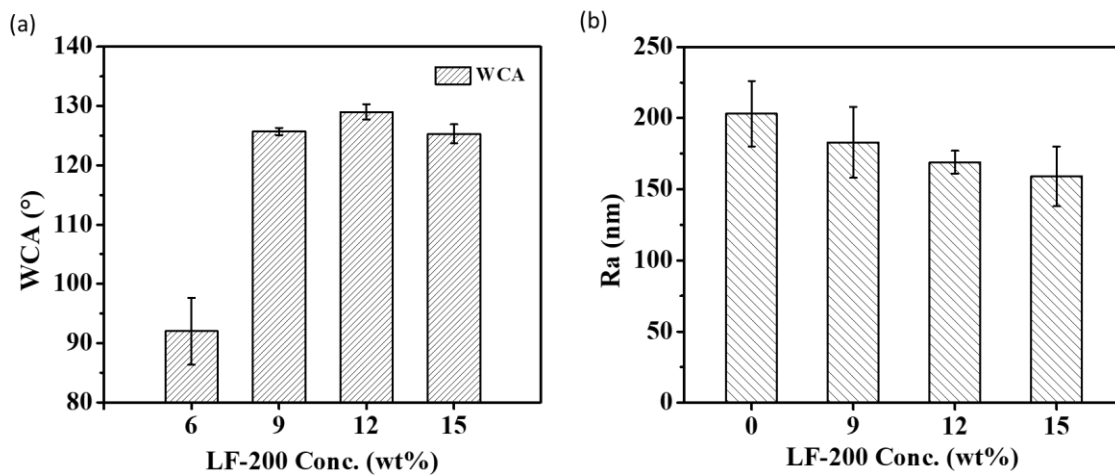
204

205 **3. Results and discussion**

206 **3.1. Hydrophobic modification of LF-200**

207 Hydrophobicity is a requisite property of MD membranes to resist the penetration of feed stream
208 into the membrane pores. In order to optimize the membrane hydrophobicity, the coating
209 solutions with a concentration of 6, 9, 12, 15 wt% LF-200 were applied to modify the NC
210 membranes. The WCAs of the respective coated membranes were compared, as shown in Fig.
211 3(a). The LF-200 concentration of 6% was too low to obtain sufficient hydrophobicity, and the
212 WCA of the modified membranes reached the peak at $129.0 \pm 1.3^\circ$ at the LF-200 concentration
213 of 12 wt%. The concentrated LF-200 coating solution had a higher viscosity, enabling more
214 polymers to attach on the membrane matrix after air-purging. However, the WCA decreased
215 when the LF-200 concentration further increased to 15 wt%. It may be owing to the impact of
216 surface roughness. As shown in Fig. 3 (b), the LF-200 coating decreased the surface roughness

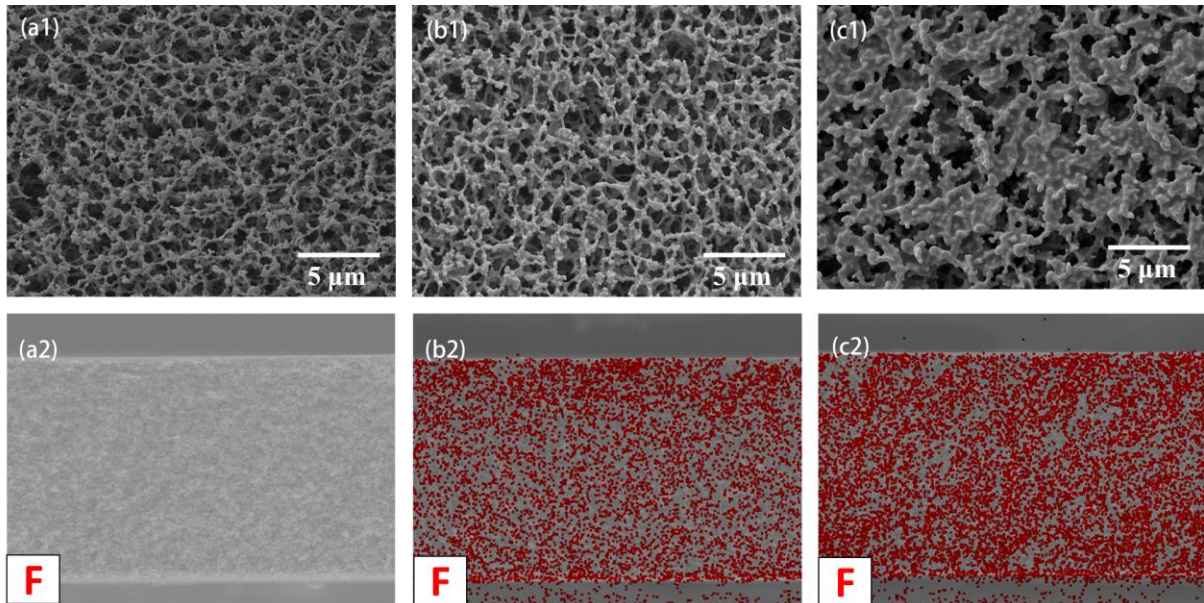
217 to some extent. It is possible that the thicker coating solution imparted 15LF-NC membrane a
218 relatively small roughness ($R_a=159$ nm), which had a negative effect on the WCA according to
219 Wenzel's theory [27]. However, all the modified membranes still had a high WCA of 125-130°,
220 thanks to the low surface energy of the coating layer.



221
222 **Fig. 3.** (a) WCAs and (b) R_a of NC membranes modified by different concentrations of LF-200.

223
224 The FESEM images of the surface morphologies and the EDX scanning of the cross-section of
225 the pristine, 9LF-NC and 12LF-NC membranes are presented in Fig. 4. The pristine NC
226 membrane matrix had a very porous and thin matrix, with no dense skin layer observed. After
227 the modification, some of the porous structures on the surface were covered and this observation
228 was more obvious in the 12LF-NC membrane as more LF-200 polymer was deposited on the
229 membrane. Nevertheless, both modified membranes still preserved porous structures, which is
230 beneficial to the mass transportation in MD. From the EDX scanning images (Fig. 4(b2) and
231 (c2)), it could be observed that the fluorine exhibited in the entire cross-section of modified

232 membrane. It means the hydrophobic modification was not only on the surface but also
233 throughout the whole membrane matrix, which was important to effectively prevent the pore
234 wetting during DCMD.

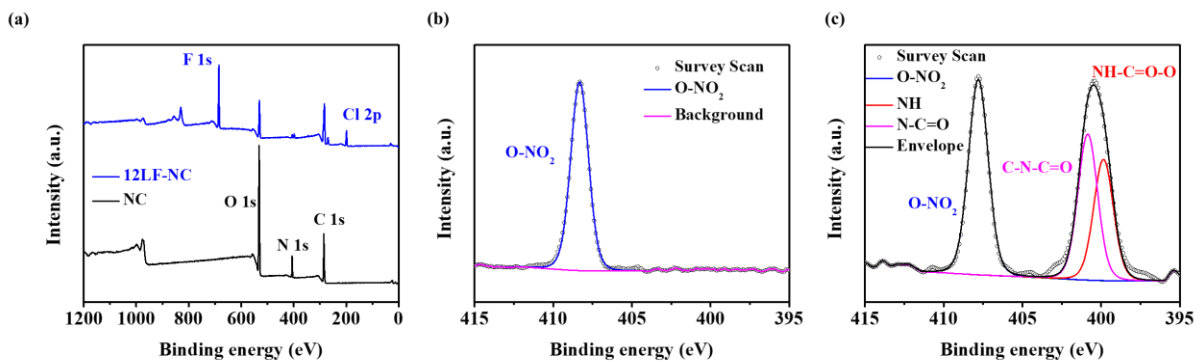


235
236 **Fig. 4.** (a1, b1, c1) FESEM images of the surface morphologies and (a2, b2, c2) the EDX spectra of
237 fluorine of cross-sections of the pristine NC, 9LF-NC and 12LF-NC membranes, respectively.

238
239 To confirm the coating of LF-200 onto the membrane and the crosslinking of the coating layer,
240 the XPS spectra of pristine NC and modified-NC membranes were compared, as shown in Fig.
241 5. From the wide spectra, it was seen that the pristine NC membrane exhibited peaks at ~285,
242 406 and 532 eV, represented the C1s, N1s and O1s in the NC compounds [28]. In the case of
243 12LF-NC membrane, besides the characteristic peaks of NC, it had extra peaks of F1s at 685
244 eV and Cl2p at 200eV because of the introduction of LF-200 onto the membrane surface.
245 Meanwhile, most of the O and N elements existed on the NC substrate was covered by the coating

246 layer so the O1s and N1s peaks decreased. In the N1s narrow spectra (Fig. 5(b) and (c)), the
 247 pristine NC membrane only showed a peak of the $-(\text{ONO}_2)$ bond at 408.3 eV [29] while the
 248 12LF-NC membrane had two extra deconvoluted peaks at 401 and 400 eV, corresponding to
 249 the N atoms in the N3300 compounds and polyurethane bonds, respectively [30, 31]. It implied
 250 the existence of a thin layer of polyurethane coating on the membrane as the NO_2 groups of the
 251 substrate still could be found. The LF-200 coating layer on the membrane can attach on the
 252 membrane surface through physical attachment since the coating has thoroughly modified the
 253 membrane matrix. In addition, the rich carboxyl groups in the polyurethane coating allow
 254 hydrogen-bonding with the acetate groups in the NC substrate [32] or amide groups in the nylon
 255 substrate [33].

256



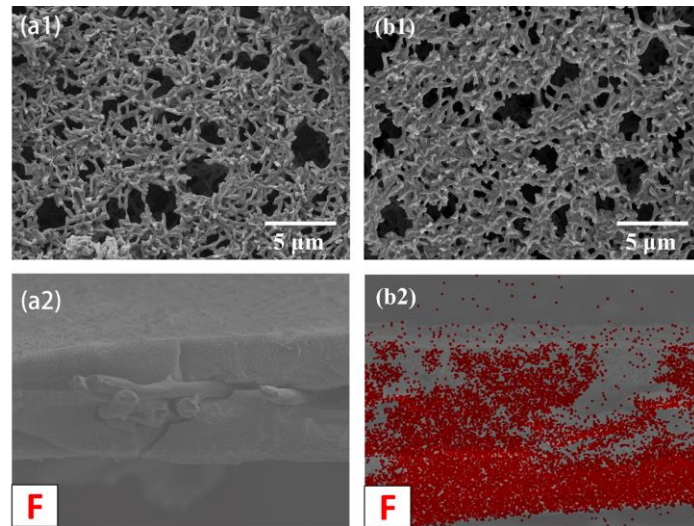
257

258 **Fig. 5.** (a) XPS wide spectra of pristine NC and modified NC membranes. N1s spectra of (b) pristine
 259 NC membrane and (c) modified NC membrane.

260

261 Aside from the NC membranes, the fluoropolymer coating was also carried out on the
 262 hydrophilic nylon membrane with LF-200 concentration of 12 wt%. Fig. 6 illustrates the surface

263 morphologies as well as the fluorine EDX spectra of the pristine nylon and 12LF-nylon
264 membranes. Similarly, the modified membrane was also covered by a thin layer of coating and
265 the matrix looked thicker, but the membrane porosity was largely preserved. At the same time,
266 the EDX spectra indicated that the modification was able to cover the entire matrix.



267
268 **Fig. 6.** (a1, b1) FESEM images of the surface morphologies and (a2, b2) the EDX spectra of fluorine of
269 cross-sections of the pristine nylon and 12LF-nylon membranes, respectively. The matrix near the
270 embedded supporting fiber was very difficult to detect so it looks blank in graph (b2).

271
272 Table 1. summarizes the WCA, LEP, thickness, pore size and porosity of pristine and modified
273 membranes. It could be seen that the modified membranes had smaller average pore sizes after
274 modification, but the decrement was very small (<10 nm). **In addition, the increment in**
275 **membrane thickness is also in the range of 1.3~3 μm after modification.** It was ascribed that the
276 air purge after dip coating removed most coating solution stuck in the pores and only left a thin
277 layer firmly affixed to the membrane matrix. Likewise, the bulk and surface porosity only

278 decreased <10% after the polymer coating. When compared to the commercial PVDF
 279 membrane, the 12LF-nylon membrane generally had a smaller porosity while the modified-NC
 280 membranes had a higher surface porosity but a lower bulk porosity.

281

282 **Table 1.** Summary of properties of the NC and nylon membranes before and after LF-200 modification.

Membrane	WCA (°)	LEP (bar)	Mean pore size (nm)	Bubble point (nm)	Thickness (μm)	Bulk porosity (%)	Surface porosity (%)
Pristine NC	0.0*	/	262±2.8	540.8±3.3	173.0±1.0	72.5±1.7	51.4±0.8
9LF-NC	125.7±0.6	2.0±0.1	257±3.8	536.0±1.1	174.3±0.6	68.1±2.3	48.4±2.0
12LF-NC	129.0±1.3	2.2±0.2	256±13.3	531.4±0.4	176.0±0.1	62.0±3.4	41.5±1.5
Nylon	0.0*	/	273.3±6.2	508.2±0.5	130.3±0.6	59.7±3.5	30.3±1.8
12LF-nylon	130.0±0.2	1.9±0.1	273.7±1.5	501.1±0.1	133.0±1.7	51.7±5.4	20.6±0.9
PVDF	130.0±0.9	2.3±0.1	230.9±3.0	513.9±4.0	210.0±0.1	75.6±3.3	37.2±4.0

283 * The water droplet completely wicked into membranes within 20 seconds.

284

285 In summary, for all the LF-200 modified membranes, the coating layer was thin and uniform
 286 all over the membranes with only a small change in the pore size and porosity. The
 287 hydrophobicity of the membranes was greatly improved from the extremely hydrophilic state.
 288 Compared to other hydrophobic modification methods conducted on hydrophilic membranes
 289 (Table 2), the LF-200 modification not only is simple (dip coating and crosslinking under low
 290 temperature), but also has a remarkable improvement in the WCA. The amount of LF-200 used
 291 for coating is much less than fabricating a whole membrane with fluoropolymer. Thus, it makes
 292 the membrane's more cost-effective and environmental-friendly. Moreover, the modification

293 method works on different substrates, including but not limited NC and nylon. Its broad
 294 applicability allows to produce MD membranes with various substrates.

295 **Table 2.** Hydrophobic coating method of hydrophilic polymeric membranes in recent literatures.

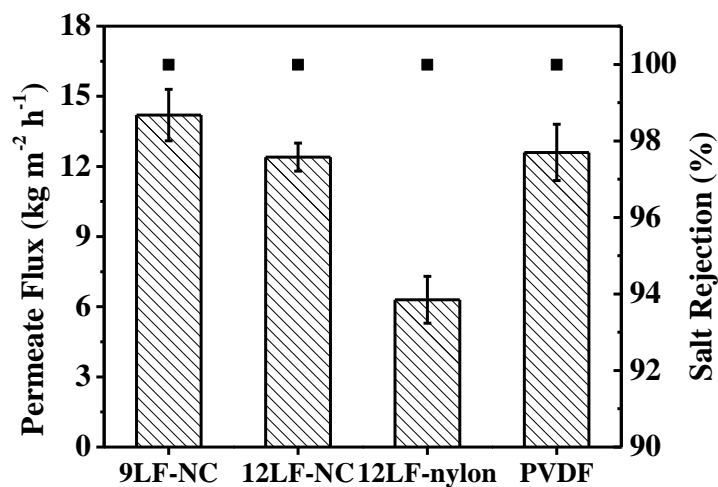
	Membrane substrate material	Coating method	WCA improvement	Ref.
Processing during membrane fabrication	PSf	Vapour-induced phase separation (VIPS)	126.0°	[24]
	PI	Electro spraying PTFE onto membrane during electrospinning	77° → 150°	[26]
	PAI or PEI	Grafting with octadecylamine	75.6° → 108°	[34]
	PAN	Plasma treatment with 1H, 1H, 2H, 2H-perfluorodecyl methacrylate	45.5° → 132.2°	[35]
	PVC	Dehydrochlorination + free radical graft copolymerization with the addition of an ethyl acrylate (EA) monomer	79° → 95°	[12]
Post-treatment to nascent membrane	PES	CF ₄ Plasma treatment	0° → 120°	[25]
	PA	UV curable Fluorolink® coating	40° → 140°	[36]
	CA	Irradiated polystyrene-grafting	96°	[37]
	NC	Plasma polymerization	115°	
	NC	LF-200 dip coating followed by thermal crosslinking	0° → 129°	This work
	Nylon		0° → 130°	

296

297 3.2. Membrane Performance in DCMD Tests

298 The modified hydrophobic membranes were applied for DCMD for desalination and their
 299 performance was first tested with 3.5 wt% NaCl feed solution for 24 h. The 9LF-NC, 12LF-
 300 NC, 12LF-nylon membranes were selected due to their high WCA and their DCMD
 301 performance was compared to the commercial PVDF membranes. Fig. 7 showed the average
 302 permeate flux and salt rejection of each membrane. During all the DCMD tests, the permeate

303 conductivity was very stable, with negligible change $<1 \mu\text{S cm}^{-1}$ after 24 h. It would be
 304 conservative to say that all membranes' rejection was nearly 100%. The fluxes of 9LF-NC,
 305 12LF-NC and PVDF membranes were $14.2, 12.1$ and $12.6 \text{ kg m}^{-2} \text{ h}^{-1}$, respectively. Among them,
 306 the 9LF-NC membrane presented a higher flux than the other two membranes because it had a
 307 smaller membrane thickness and low wettability (Table.1), which were beneficial to mass
 308 transfer. It also had a slightly larger pore size and surface porosity to provide larger area for
 309 water vapor evaporation [9, 17]. Meanwhile, the 12LF-NC membrane also had a similar flux
 310 with PVDF, contributed by its smaller thickness, slightly larger pore size and surface porosity.
 311 In case of the 12LF-nylon membrane, the effect of low porosity was very obvious. Even though
 312 it possessed a similar WCA and a small thickness compared with other membranes, it exhibited
 313 a much lower flux of $6.3 \text{ kg m}^{-2} \text{ h}^{-1}$. Considering the relatively lower flux of 12LF-nylon
 314 membrane, the following study will only put the emphasis on the modified NC membranes.

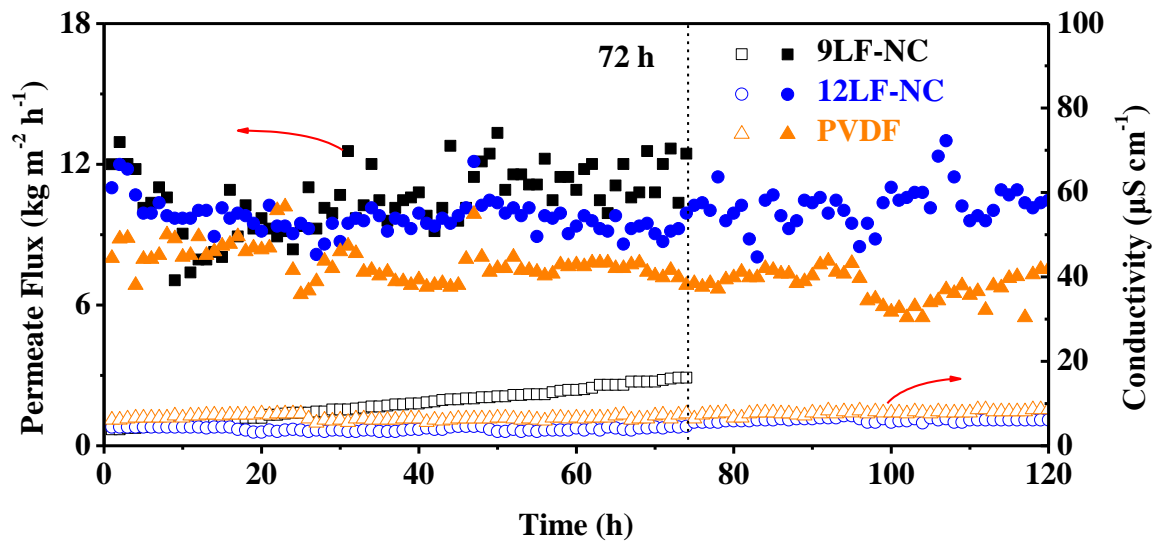


315
 316 **Fig. 7.** DCMD performances of the 9LF-NC, 12LF-NC, 12LF-nylon and commercial PVDF membranes
 317 in 3.5 wt% NaCl solution.

318

319 The 9LF-NC, 12LF-NC and commercial PVDF membranes were continued in long-term
320 DCMD experiments feeding with 10 wt% NaCl. The desalination of feed solution with such a
321 high osmotic pressure (~84 bar) is a dilemma to RO process. However, the constraint can be
322 overcome by MD process since it is insensitive to the feed's osmotic pressure. Fig. 8 depicts
323 the permeate flux and the permeate conductivity over time. The DCMD performance of both of
324 PVDF and 12LF-NC membranes were stable over 120 hours, with a very slightly increment in
325 the permeate conductivity. Their flux both decreased compared to the performance in 3.5 wt%
326 NaCl. This was because the higher salt concentration could cause more severe concentration
327 polarization and pose more mass transfer resistance [38]. Surprisingly, the flux decrement of
328 12LF-NC membrane (18.5%) was lower than PVDF membrane (38.8%). It may be related to
329 the different structures and properties of membrane substrates, such as surface porosity, leading
330 to a different concentration polarization degree and different driving forces in DCMD. For the
331 9LF-NC membrane, it was not as durable as the 12LF-NC membrane though it did work well
332 in the baseline test. The increasing permeate conductivity from 3.9 to 16.1 $\mu\text{S cm}^{-1}$ after 74 h
333 showed a sign of salt leakage from the feed side to the permeate side. The salt leakage in MD
334 process can be caused by either the small droplet entrained in water vapour or membrane pore
335 wetting [39]. As the flux of 9LF-NC membrane did not rise up significantly, it may not be
336 conclusive that the membrane pores were fully wetted. Some fine liquid droplets may be carried

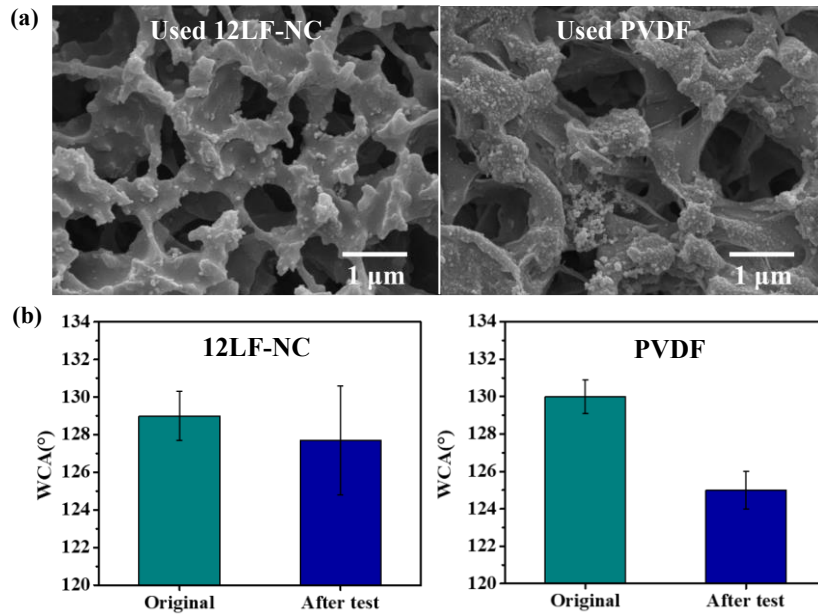
337 in the vapour phase, given that the lower WCA and water repellence of the membranes [39].



338
339 **Fig. 8.** Long-term DCMD performances of the 9LF-NC, 12LF-NC and commercial PVDF membranes
340 with 10 wt% NaCl feed solution.

341
342 To study the stability of the hydrophobic coating, the surface morphologies and WCAs of the
343 12LF-NC and PVDF membranes were tested again after the long-term DCMD experiments. As
344 shown in Fig. 9(a), there were fewer NaCl crystals found on the surface of 12LF-NC membrane
345 facing the feed stream than the commercial PVDF membrane. A possible reason of the fewer
346 inorganic fouling could be the higher surface porosity of 12LF-NC membrane, which could
347 induce a larger area of air-water interface near the membrane interface and decrease the
348 possibility of scalants adsorption onto the membrane surface [40]. Besides, the WCA of the
349 modified membrane after 144 hours DCMD run remained at a high value of $127.7 \pm 2.9^\circ$.
350 Compared to the commercial PVDF membrane, the decrement was much smaller. This result

351 was a good proof of the persistence of the coating layer and the sufficient adhesion between the
352 coating and substrates.



353
354 **Fig. 9.** (a). FESEM images of the used 12LF-NC and PVDF membranes after long-term DCMD
355 experiments fed with 10 wt% NaCl solution. (b) WCAs of 12LF-NC and PVDF membranes measured
356 before and after test, respectively.

357
358 Table 3 compares the MD performance of the LF-200 coated NC membranes with other flat
359 sheet membranes. Both the 9LF-NC and 12LF-NC membranes have an almost perfect rejection
360 when treating 3.5% NaCl feed, which outperformed many commercial hydrophobic polymeric
361 membranes. Compared to other modified membranes, the LF-200 coated NC membranes is still
362 very competitive in permeation flux and rejection considering its facile modification process.
363 Furthermore, in the case of 10 wt% NaCl feed solution, the 12LF-NC membrane showed an
364 outstanding performance over 120 h while most of the other membranes were only challenged
365 with a lower NaCl concentration for a short time. Its durability allows its application in the

366 brine water that has high salinity and make good use of the unique character of MD.

Table 3. The DCMD performance of modified membranes in this work compared with other membranes in recent literatures.

Membrane type	Membrane	WCA (°)	Feed/ Temperature (°C)	Permeate NaCl conc. (wt%)	Permeate Flux (kg m ⁻² h ⁻¹)	Performance	Ref.
Made of hydrophobic polymer	PVDF (co-casting)	~130.0	60/20	3.5	24.0	Conductivity increase from 7 to 10 μ S/cm within 48 h	[41]
	PVDF-HFP	89.3	60/18.5	3.5	16.1	99.3%	[42]
	PVDF (Millipore, GVHP)	120.0	59/20	3.5	8.4	/	[43]
				10	3.7	/	
	PTFE (CHMLAB)	114.0	60/20	3.5	13.0	>99.97%	[38]
PVDF (Merck Millipore)	130.0	60/20	3.5	12.6	Stable conductivity	This work	
			10.0	7.7			
Made of hydrophilic polymer	PSf (VIPs)	106.4	73/25	3.5	30.0	Nearly 100% for 90 h	[24]
	PA modified by PFPE	140.0	50/15	3.5	11.0	99.6% for 12 h	[36]
	DHPVC-g-PEA	90.0	65/20	3.5	19.3	99.94%, 80 h	[12]
	Polystyrene-grafted CA	78.4	60/25	2.9	2.4	99.1%	[37]
	Vinyltrimethylsilicon/CF ₄ plasma-treated NC	~115.0	70/25	2.9	30.3	99.9%	
	9LF-NC	125.0	60/20	3.5	14.0	Nearly 100% for 24 h	This work
	12LF-NC	129.0	60/20	3.5	12.1	Nearly 100% for 24 h	
				10.0	10.1	Stable conductivity over 120 h	

4. Conclusions

This work successfully developed a facile hydrophobic modification method that could transform the originally hydrophilic NC and nylon membranes into hydrophobic membranes. FEVE polymer was coated on the entire surface of the membrane matrix through a simple dip coating approach, and crosslinking of the polymer was carried out via low temperature heat treatment. The modified membranes have high WCA ($>125^\circ$) and LEP (~ 2 bar), with their porous microstructure largely preserved. The membranes are applicable in DCMD, treating high-salinity feed solutions with NaCl concentration up to 10 wt%. The 12LF-NC membrane showed excellent flux of $10.1 \text{ kg m}^{-2} \text{ h}^{-1}$ in the treatment of 10 wt% salt water, which is 31% higher than the commercial PVDF membrane. Also, the conductivity was stable over 120 h, showing no sign of membrane wetting. The good MD performance is attributed by the highly porous structure of the pristine hydrophilic membrane and the uniform hydrophobic layer throughout the matrix imparted by the FEVE coating. In comparison to other hydrophobic modification method, this method is superior in the facile operation and versatility in different hydrophilic substrates without the use of plasma or irradiation. The remarkable performance of 12LF-NC membrane also strongly elucidates the potential of the MD membranes for the treatment of high-salinity water.

Acknowledgements

The authors would like to acknowledge the research scholarship provided by Interdisciplinary Graduate Programme, Nanyang Technological University and the funding support from the Singapore Economic Development Board to the Singapore Membrane Technology Centre, Nanyang Environment & Water Research Institute at Nanyang Technological University, Singapore.

References

- [1] Y.J. Lim, K. Goh, M. Kurihara, R. Wang, Seawater desalination by reverse osmosis: Current development and future challenges in membrane fabrication – A review, *J Membrane Sci* 629 (2021) 119292. <https://doi.org/https://doi.org/10.1016/j.memsci.2021.119292>.
- [2] E. Jones, M. Qadir, M.T.H. van Vliet, V. Smakhtin, S.-m. Kang, The state of desalination and brine production: A global outlook, *Science of The Total Environment* 657 (2019) 1343-1356. <https://doi.org/https://doi.org/10.1016/j.scitotenv.2018.12.076>.
- [3] C. Li, X. Li, X. Du, Y. Zhang, W. Wang, T. Tong, A.K. Kota, J. Lee, Elucidating the Trade-off between Membrane Wetting Resistance and Water Vapor Flux in Membrane Distillation, *Environmental Science & Technology* 54(16) (2020) 10333-10341. <https://doi.org/10.1021/acs.est.0c02547>.
- [4] J. Wu, B. Jung, A. Anvari, S. Im, M. Anderson, X. Zheng, D. Jassby, R.B. Kaner, D. Dlamini, A. Edalat, E.M.V. Hoek, Reverse osmosis membrane compaction and embossing at ultra-high pressure operation, *Desalination* 537 (2022) 115875. <https://doi.org/https://doi.org/10.1016/j.desal.2022.115875>.
- [5] K.M. Shah, I.H. Billinge, X. Chen, H. Fan, Y. Huang, R.K. Winton, N.Y. Yip, Drivers, challenges, and emerging technologies for desalination of high-salinity brines: A critical review, *Desalination* 538 (2022) 115827. <https://doi.org/https://doi.org/10.1016/j.desal.2022.115827>.
- [6] N.A. Pham, D.Y.F. Ng, K. Goh, Z. Dong, R. Wang, Assessing the potential of integrally skinned asymmetric hollow fiber membranes for addressing membrane fouling in pressure retarded osmosis process, *Desalination* 520 (2021) 115347.
- [7] V. Karanikola, C. Boo, J. Rolf, M. Elimelech, Engineered Slippery Surface to Mitigate Gypsum Scaling in Membrane Distillation for Treatment of Hypersaline Industrial Wastewaters, *Environmental Science & Technology* 52(24) (2018) 14362-14370. <https://doi.org/10.1021/acs.est.8b04836>.
- [8] N.G.P. Chew, Y. Zhang, K. Goh, J.S. Ho, R. Xu, R. Wang, Hierarchically structured Janus membrane surfaces for enhanced membrane distillation performance, *ACS Applied Materials & Interfaces* 11(28) (2019) 25524-25534.
- [9] Y. Zhang, J.Y. Chong, R. Xu, R. Wang, Hydrophobic ceramic membranes fabricated via fatty acid chloride modification for solvent resistant membrane distillation (SR-MD), *Journal of Membrane Science* (2022) 120715.
- [10] G. Tan, D. Xu, Z. Zhu, X. Zhang, J. Li, Tailoring pore size and interface of superhydrophobic nanofibrous membrane for robust scaling resistance and flux enhancement in membrane distillation, *Journal of Membrane Science* 658 (2022) 120751. <https://doi.org/https://doi.org/10.1016/j.memsci.2022.120751>.
- [11] H. Li, H. Feng, M. Li, X. Zhang, Engineering a covalently constructed superomniphobic

- membrane for robust membrane distillation, *Journal of Membrane Science* 644 (2022) 120124. <https://doi.org/https://doi.org/10.1016/j.memsci.2021.120124>.
- [12] S.S. Hussein, S.S. Ibrahim, M.A. Toma, Q.F. Alsahy, E. Drioli, Novel chemical modification of polyvinyl chloride membrane by free radical graft copolymerization for direct contact membrane distillation (DCMD) application, *J Membrane Sci* 611 (2020) 118266.
- [13] J. Meng, C.H. Lau, Y. Xue, R. Zhang, B. Cao, P. Li, Compatibilizing hydrophilic and hydrophobic polymers via spray coating for desalination, *Journal of Materials Chemistry A* 8(17) (2020) 8462-8468.
- [14] M. Xu, J. Cheng, X. Du, Q. Guo, Y. Huang, Q. Huang, Amphiphobic electrospun PTFE nanofibrous membranes for robust membrane distillation process, *Journal of Membrane Science* 641 (2022) 119876. <https://doi.org/https://doi.org/10.1016/j.memsci.2021.119876>.
- [15] Y. Zhang, Y. Peng, S. Ji, Z. Li, P. Chen, Review of thermal efficiency and heat recycling in membrane distillation processes, *Desalination* 367 (2015) 223-239. <https://doi.org/10.1016/j.desal.2015.04.013>.
- [16] J.F. Kim, J.H. Kim, Y.M. Lee, E. Drioli, Thermally induced phase separation and electrospinning methods for emerging membrane applications: A review, *AIChE Journal* 62(2) (2016) 461-490.
- [17] Y. Zhang, J.Y. Chong, R. Xu, R. Wang, Effective separation of water-DMSO through solvent resistant membrane distillation (SR-MD), *Water Research* 197 (2021) 117103. <https://doi.org/https://doi.org/10.1016/j.watres.2021.117103>.
- [18] S. Feng, Z. Zhong, Y. Wang, W. Xing, E. Drioli, Progress and perspectives in PTFE membrane: Preparation, modification, and applications, *J Membrane Sci* 549 (2018) 332-349. <https://doi.org/https://doi.org/10.1016/j.memsci.2017.12.032>.
- [19] Y. Huang, Q.-L. Huang, H. Liu, C.-X. Zhang, Y.-W. You, N.-N. Li, C.-F. Xiao, Preparation, characterization, and applications of electrospun ultrafine fibrous PTFE porous membranes, *Journal of Membrane Science* 523 (2017) 317-326. <https://doi.org/https://doi.org/10.1016/j.memsci.2016.10.019>.
- [20] C. Su, Y. Li, H. Cao, C. Lu, Y. Li, J. Chang, F. Duan, Novel PTFE hollow fiber membrane fabricated by emulsion electrospinning and sintering for membrane distillation, *Journal of Membrane Science* 583 (2019) 200-208. <https://doi.org/https://doi.org/10.1016/j.memsci.2019.04.037>.
- [21] T. Zhou, Y. Yao, R. Xiang, Y. Wu, Formation and characterization of polytetrafluoroethylene nanofiber membranes for vacuum membrane distillation, *Journal of Membrane Science* 453 (2014) 402-408.
- [22] E. Giannetti, Semi-crystalline fluorinated polymers, *Polymer international* 50(1) (2001) 10-26.
- [23] S. Dolui, D. Kumar, S. Banerjee, B. Ameduri, Well-Defined Fluorinated Copolymers: Current Status and Future Perspectives, *Accounts of Materials Research* 2(4) (2021) 242-251.

<https://doi.org/10.1021/accountsmr.1c00015>.

[24] Y. Peng, Y. Dong, H. Fan, P. Chen, Z. Li, Q. Jiang, Preparation of polysulfone membranes via vapor-induced phase separation and simulation of direct-contact membrane distillation by measuring hydrophobic layer thickness, *Desalination* 316 (2013) 53-66.

<https://doi.org/https://doi.org/10.1016/j.desal.2013.01.021>.

[25] X. Wei, B. Zhao, X.-M. Li, Z. Wang, B.-Q. He, T. He, B. Jiang, CF₄ plasma surface modification of asymmetric hydrophilic polyethersulfone membranes for direct contact membrane distillation, *J Membrane Sci* 407-408 (2012) 164-175.

<https://doi.org/https://doi.org/10.1016/j.memsci.2012.03.031>.

[26] J. Ju, Z. Li, Y. Lv, M. Liu, K. Fejjari, W. Kang, Y. Liao, Electrospun PTFE/PI bi-component membranes with robust 3D superhydrophobicity and high water permeability for membrane distillation, *J Membrane Sci* 611 (2020) 118420.

<https://doi.org/https://doi.org/10.1016/j.memsci.2020.118420>.

[27] R.N. Wenzel, RESISTANCE OF SOLID SURFACES TO WETTING BY WATER, *Industrial & Engineering Chemistry* 28(8) (1936) 988-994. <https://doi.org/10.1021/ie50320a024>.

[28] Q. Luo, T. Ren, H. Shen, J. Zhang, D. Liang, The thermal properties of nitrocellulose: from thermal decomposition to thermal explosion, *Combustion Science and Technology* 190(4) (2018) 579-590.

[29] K. Yoshihara, A. Tanaka, Interlaboratory study on the degradation of poly (vinyl chloride), nitrocellulose and poly (tetrafluoroethylene) by x-rays in XPS, *Surface and Interface Analysis: An International Journal devoted to the development and application of techniques for the analysis of surfaces, interfaces and thin films* 33(3) (2002) 252-258.

[30] T. Vieira, J. Carvalho Silva, A.M. Botelho do Rego, J.P. Borges, C. Henriques, Electrospun biodegradable chitosan based-poly(urethane urea) scaffolds for soft tissue engineering, *Materials Science and Engineering: C* 103 (2019) 109819.

<https://doi.org/https://doi.org/10.1016/j.msec.2019.109819>.

[31] A.A. Qaiser, M.M. Hyland, X-ray photoelectron spectroscopy characterization of polyaniline-cellulose ester composite membranes, *Materials Science Forum, Trans Tech Publ*, 2010, pp. 35-45.

[32] E. Yilgör, İ. Yilgör, E. Yurtsever, Hydrogen bonding and polyurethane morphology. I. Quantum mechanical calculations of hydrogen bond energies and vibrational spectroscopy of model compounds, *Polymer* 43(24) (2002) 6551-6559.

[https://doi.org/https://doi.org/10.1016/S0032-3861\(02\)00567-0](https://doi.org/https://doi.org/10.1016/S0032-3861(02)00567-0).

[33] Y. Fukuda, K. Miyamae, Y. Sasanuma, Computational design of polymers: poly (ester amide) and polyurethane, *RSC advances* 7(61) (2017) 38387-38398.

[34] Y. Zhang, R. Wang, L. Zhang, A.G. Fane, Novel single-step hydrophobic modification of polymeric hollow fiber membranes containing imide groups: Its potential for membrane contactor application, *Sep Purif Technol* 101 (2012) 76-84.

<https://doi.org/https://doi.org/10.1016/j.seppur.2012.09.009>.

[35] L. Liu, F. Shen, X. Chen, J. Luo, Y. Su, H. Wu, Y. Wan, A novel plasma-induced surface hydrophobization strategy for membrane distillation: Etching, dipping and grafting, *J Membrane Sci* 499 (2016) 544-554.

[36] A. Figoli, C. Ursino, F. Galiano, E. Di Nicolò, P. Campanelli, M.C. Carnevale, A. Criscuoli, Innovative hydrophobic coating of perfluoropolyether (PFPE) on commercial hydrophilic membranes for DCMD application, *J Membrane Sci* 522 (2017) 192-201.

<https://doi.org/https://doi.org/10.1016/j.memsci.2016.08.066>.

[37] Y. Wu, Y. Kong, X. Lin, W. Liu, J. Xu, Surface-modified hydrophilic membranes in membrane distillation, *Journal of Membrane Science* 72(2) (1992) 189-196.

[https://doi.org/https://doi.org/10.1016/0376-7388\(92\)80199-T](https://doi.org/https://doi.org/10.1016/0376-7388(92)80199-T).

[38] N.A.M. Ameen, S.S. Ibrahim, Q.F. Alsalhy, A. Figoli, Highly Saline Water Desalination Using Direct Contact Membrane Distillation (DCMD): Experimental and Simulation Study, *Water* 12(6) (2020). <https://doi.org/10.3390/w12061575>.

[39] M. Rezaei, D.M. Warsinger, W.M. Samhaber, Wetting prevention in membrane distillation through superhydrophobicity and recharging an air layer on the membrane surface, *J Membrane Sci* 530 (2017) 42-52.

[40] L. Liu, Z. Xiao, Y. Liu, X. Li, H. Yin, A. Volkov, T. He, Understanding the fouling/scaling resistance of superhydrophobic/omniphobic membranes in membrane distillation, *Desalination* 499 (2021) 114864.

[41] M. Tian, J. Zhu, S. Yuan, Y. Zhang, B. Van der Bruggen, A co-casting route enables the formation of skinless, hydrophobic poly (vinylidene fluoride) membranes for DCMD, *J Membrane Sci* 630 (2021) 119299.

[42] S. Fadhil, T. Marino, H.F. Makki, Q.F. Alsalhy, S. Blefari, F. Macedonio, E.D. Nicolò, L. Giorno, E. Drioli, A. Figoli, Novel PVDF-HFP flat sheet membranes prepared by triethyl phosphate (TEP) solvent for direct contact membrane distillation, *Chemical Engineering and Processing: Process Intensification* 102 (2016) 16-26.

<https://doi.org/https://doi.org/10.1016/j.cep.2016.01.007>.

[43] R. Bouchrit, A. Boubakri, A. Hafiane, S.A.-T. Bouguecha, Direct contact membrane distillation: Capability to treat hyper-saline solution, *Desalination* 376 (2015) 117-129.

<https://doi.org/https://doi.org/10.1016/j.desal.2015.08.014>.